

Crystallization of the chalcogenide compound Sb_8Te_3

Kouichi Kifune,^{a,b*} Tomoko Fujita,^b Yoshiki Kubota,^b Noboru Yamada^c and Toshiyuki Matsunaga^d

^aFaculty of Liberal Arts and Sciences, Osaka Prefecture University, Japan, ^bGraduate School of Science, Osaka Prefecture University, Japan, ^cAV Core Technology Development Center, Panasonic Corporation, Japan, and ^dMaterials Science and Analysis Technology Center, Panasonic Corporation, Japan

Correspondence e-mail:
kifune@las.osakafu-u.ac.jp

Received 4 May 2011
Accepted 18 August 2011

The crystallization of a sputtered Sb_8Te_3 film was examined in an X-ray powder diffraction experiment. An as-sputtered, amorphous Sb_8Te_3 film crystallized during heating into a structure of Sb–Te homologous series modulated along the stacking direction. During heating the lattice parameters and the modulation period γ were found to change significantly and continuously; this observation suggests a continuous change in the stacking sequence. A superspace analysis revealed that with heating the modulation period γ increased to a value that seemed to be determined by the atomic composition. Once γ reached this value it remained unchanged with cooling. A three-dimensional projection of the converged four-dimensional superspace structure corresponded to the homologous Sb_8Te_3 structure.

1. Introduction

Phase change recording, which exploits a reversible phase change between the amorphous and crystalline states of a material, is extensively used for non-volatile and rewritable memory in videodisc recorders, mobile phones and computers. The most commonly used recording materials are GeTe– Sb_2Te_3 pseudobinary compounds and Sb–Te binary compounds containing a small quantity of In, Ag and/or Ge. These compounds have superior data retention at room temperature for extended periods and high rewrite speeds (Yamada & Matsunaga, 2000; Matsunaga *et al.*, 2001, 2004, 2011; Matsunaga & Yamada, 2004).

It has been found that in thermal equilibrium, the GeTe– Sb_2Te_3 pseudobinary and Sb–Te binary systems form various intermetallic compounds represented by the chemical formula $(\text{GeTe})_n(\text{Sb}_2\text{Te}_3)_m$ and $(\text{Sb}_2)_n(\text{Sb}_2\text{Te}_3)_m$ (n, m : integer). All of these structures, which are called homologous phases, have similar trigonal structures that are characterized by a stacking of NaCl-type blocks along the c_h axis with very long cell dimensions in their conventional three-dimensional structural description (Karpinsky *et al.*, 1998; Shelimova *et al.*, 2000, 2001; Poudeu & Kanatzidis, 2005; Matsunaga *et al.*, 2007, 2008, 2010). We analyzed the crystal structure of sufficiently annealed Sb_8Te_3 in the conventional three-dimensional formalism, revealing that this compound has an $11R$ – $(\text{Sb}_2)_3(\text{Sb}_2\text{Te}_3)_1$ structure, as expected from its chemical formula (Kifune *et al.*, 2005; Matsunaga *et al.*, 2010).

However, it has been reported that in Bi–Te and Bi–Se binary systems, both commensurate and incommensurate structures are present (Lind & Lidin, 2003). These investigations imply that the Sb–Te system could also have an incommensurate modulated structure characterized by the modulation vector $\mathbf{q} = \gamma \cdot \mathbf{c}^*$, where γ is an irrational number and \mathbf{c}^* is the fundamental reciprocal vector formed by the

three-layer cubic stacking. We therefore re-examined the crystal structure in detail using an as-deposited Sb_8Te_3 film. This report examines the structural changes that occurred with changing specimen temperature.

2. Experimental

A thin film specimen was formed on a quartz glass substrate by DC sputtering using an Sb–Te alloy target in an Ar gas atmosphere. The composition of the Sb–Te film was Sb:Te = 71.5:28.5, as measured by electron probe micro-analysis (EPMA) using a Jeol JXA-8900R instrument. A powder specimen was produced for the X-ray measurements by scraping the disk surface with a spatula, and then packing the scrapings into a quartz capillary tube with an internal diameter of 0.3 mm. The opening of the capillary was sealed using an oxyacetylene flame to insulate the powder specimen from the atmosphere. The X-ray diffraction experiments were carried out using a Debye–Scherrer camera with an imaging plate at the Japan Synchrotron Radiation Research Institute BL02B2 beamline (Nishibori *et al.*, 2001). The wavelength of the incident beam was $\lambda = 0.4209 \text{ \AA}$. The temperature of the specimen

was adjusted by blowing high-temperature N_2 gas over the capillary. The collection of diffraction intensity data was carried out as follows: first the sample was exposed to X-rays for 5 min at room temperature, then it was heated to a preset temperature and held for 2 min for the temperature to stabilize. Diffraction data were then collected during a 5 min exposure at this temperature. This process was carried out continuously at intervals of 20–100 K up to 831 K (see legend to Fig. 1). The cooling process was similar and the temperature was lowered from 831 to 300 K. Data analyses of the powder diffraction profiles were performed by applying the four-dimensional superspace formalism using *JANA2000* (Petříček & Dušek, 2000).

3. Results and discussion

X-ray powder diffraction patterns measured *in situ* while changing the specimen temperature are shown in Fig. 1. During the heating process (Fig. 1*a*) these profiles indicated that the as-sputtered Sb_8Te_3 specimen was in an amorphous state at room temperature, but crystallized with heating into a

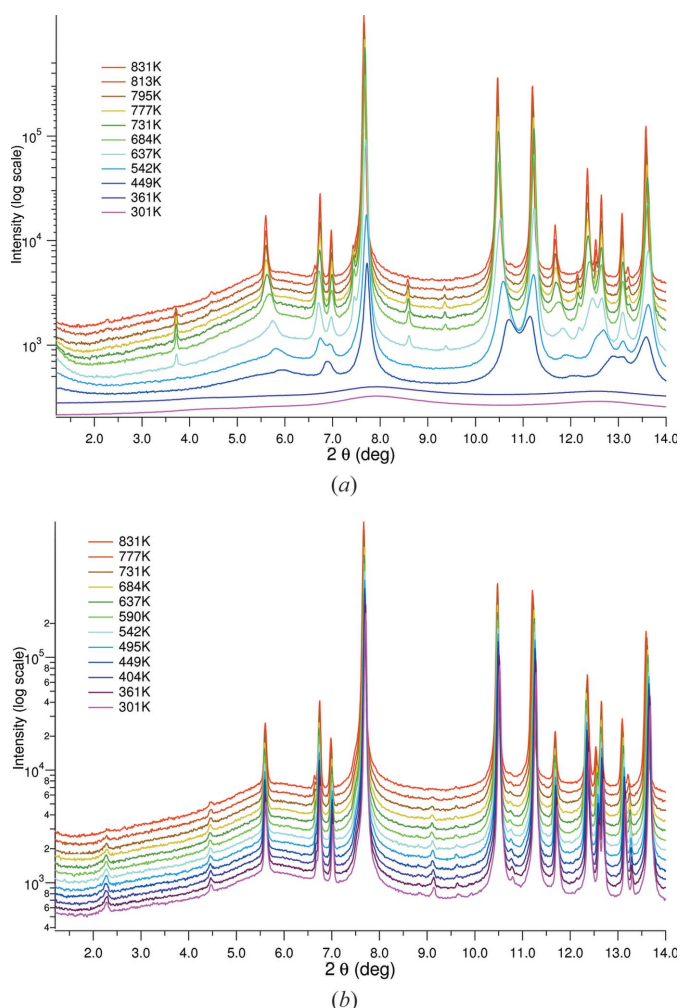


Figure 1 Temperature dependence of the X-ray powder diffraction profiles of an Sb_8Te_3 powder specimen: (a) heating process; (b) cooling process.

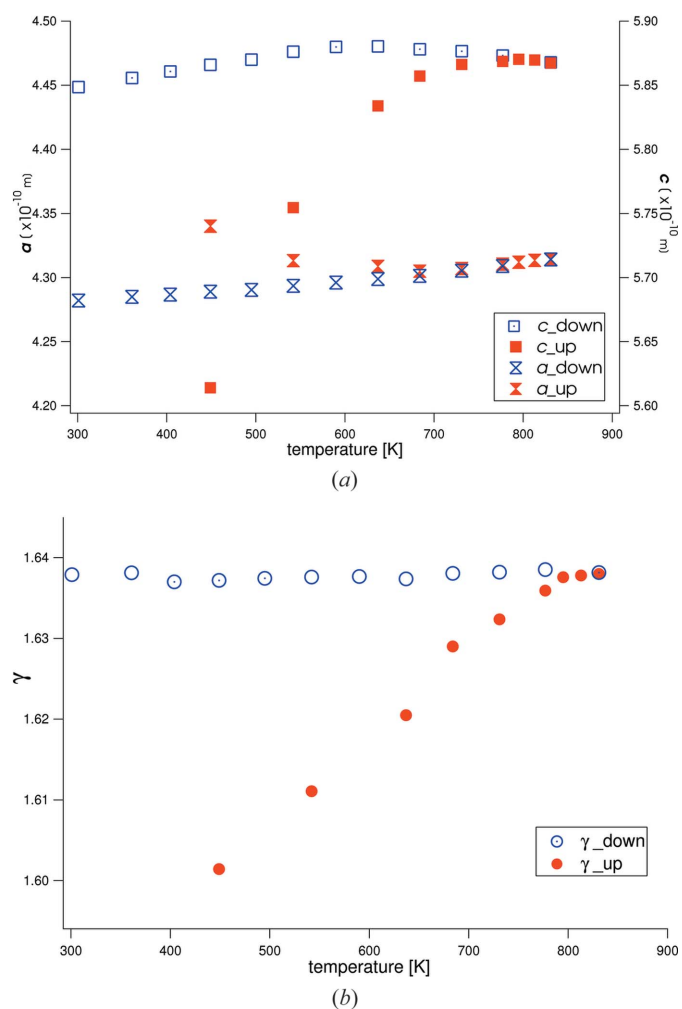


Figure 2 Temperature dependences of lattice parameters, (a) a and c , and (b) the modulation period γ value from a four-dimensional Le Bail fitting. Error bars were omitted because they were smaller than the symbols shown.

Table 1

Experimental details.

Crystal data	
Chemical formula	Sb ₈ Te ₃
M_r	1356.8
Crystal system, space group	Trigonal, $R\bar{3}m(00\gamma)$
Temperature	831
Wave vectors	$\mathbf{q} = 1.63774\mathbf{c}^*$
a, c (Å)	4.3134, 5.8658
V (Å ³)	94.51
Z	1
Radiation type	Synchrotron, $\lambda = 0.4209$ Å
Specimen shape, size (mm)	Cylinder, 3.0×0.3
Data collection	
Diffractometer	Debye–Scherrer camera
Specimen mounting	Sealed quartz capillary tube
Data collection mode	Transmission
Scan method	Fixed
2θ values (°)	$2\theta_{\min} = 1.2, 2\theta_{\max} = 39, 2\theta_{\text{step}} = 0.01$
Refinement	
R factors and goodness-of-fit	$R_p = 0.032, R_{\text{wp}} = 0.046, R_{\text{exp}} = 0.024,$ $R(F) = 0.062, \chi^2 = \text{not found}$
No. of data points	3781
No. of parameters	51
No. of restraints	0
$\Delta\rho_{\max}$ (e Å ⁻³)	0.481

Computer programs used: JANA2000 (Petříček & Dušek, 2000).

transient homologous structure close to the A7-type. This structure is based on the stacking of three cubic close-packed layers. As shown in Fig. 1(a), the superlattice diffraction lines with diffraction angles from 5 to 7° in 2θ on the lower angle side of the strongest fundamental line shifted markedly with increasing temperature. On the other hand, during the cooling process (Fig. 1b) the profiles remained relatively unchanged.

Four-dimensional Le Bail analysis of all diffraction data except for the amorphous data at 301 and 361 K was performed using the program JANA2000. The structure model

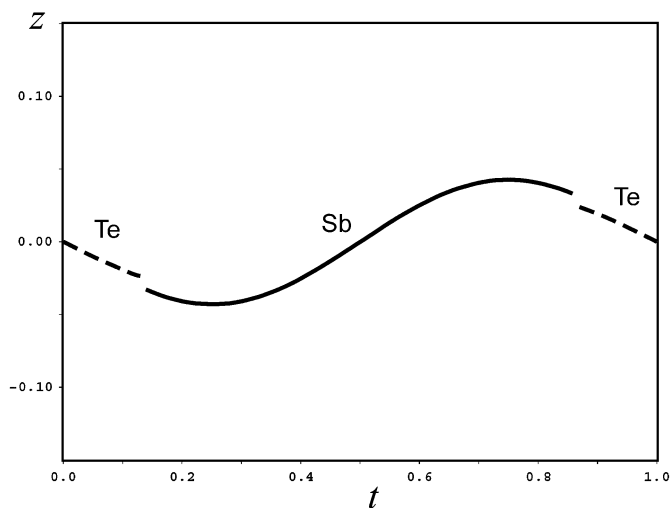


Figure 3

The z -parameter modulations of atomic position versus the internal parameter t at 831 K (Sb: solid line, Te: broken line). The modulation in the displacement of the two atoms in this binary alloy can be described relatively well by a single trigonometric function.

Table 2

Crystal data and refinement results for the four-dimensional model of Sb₈Te₃ at 831 K.

The diffraction data used for the analysis was: $1.20 \leq 2\theta \leq 39.00^\circ$. The superspace group was $P:R\bar{3}m:\bar{1}1$. B_1^S indicates the amplitude of the sine displacement wave.

Atom	x	y	z	B_1^S	U_{iso} (Å ²)
Sb	0	0	0	−0.0427 (3)	0.0551 (4)
Te	0	0	0	−0.033 (2)	0.0294 (5)
R-factors of profile and all reflections					
				R_p	0.032
				R_{wp}	0.046
				RF_{obs}	0.056
				wRF_{obs}	0.026
R-factors of main and satellite reflections					
Main					
				RF_{obs}	0.030
				wRF_{obs}	0.012
R-factors of satellites					
1st order					
				RF_{obs}	0.067
				wRF_{obs}	0.051
2nd order					
				RF_{obs}	0.108
				wRF_{obs}	0.031
3rd order					
				RF_{obs}	0.091
				wRF_{obs}	0.043

for this analysis was as follows: the superspace group was $P:R\bar{3}m:\bar{1}1$, the basic unit cell consisted of three cubic close-packed layers, and modulation of the atomic displacement was characterized by a single modulation vector $\mathbf{q} = \gamma \cdot \mathbf{c}^*$. The lattice parameters a and c obtained for the fundamental structure, and γ of the modulation period, are plotted in Fig. 2 for every measurement temperature. When temperature increased, the magnitude of a did not change greatly. On the other hand, c changed considerably from 5.60 to 5.86 Å (Fig. 2a). In Fig. 2(b) the γ value is close to 1.60 at 449 K and increases with increasing temperature, finally reaching 1.637 at 795 K. This is the same within experimental error as the expected value of $18/11 = 1.636$ based on the commensurate 11-layer structure of Sb₈Te₃, which is present at 27.27 at% Te composition. During the cooling process a, c and γ remained nearly constant. Therefore, this structural transformation can be considered irreversible. Since the γ value of 1.60 corresponds to the 15-layer (Sb₂)₅(Sb₂Te₃)₁ structure (Matsunaga *et al.*, 2010), the as-sputtered Sb–Te specimen was presumed to crystallize from the amorphous phase to an A7-type fundamental structure ($\gamma = 1.5$), initially with a highly disordered atomic arrangement of Sb and Te. We have also found that γ of some other Sb–Te amorphous films had values close to 1.5 just after the transformation to each crystalline phase. In an Ag_{3.5}In_{3.8}Sb_{75.0}Te_{17.7} specimen formed by adding small amounts of In and Ag to an Sb–Te binary compound, it was demonstrated that a distorted octahedral structure formed by three short and three long Sb–Sb bonds is present in both the amorphous phase and the A7-type crystal phase, and that this distorted structure plays a fundamental role in a rapid structural transformation (Matsunaga *et al.*, 2011). Furthermore, as seen in Fig. 2(b), the γ value rose continuously with increasing

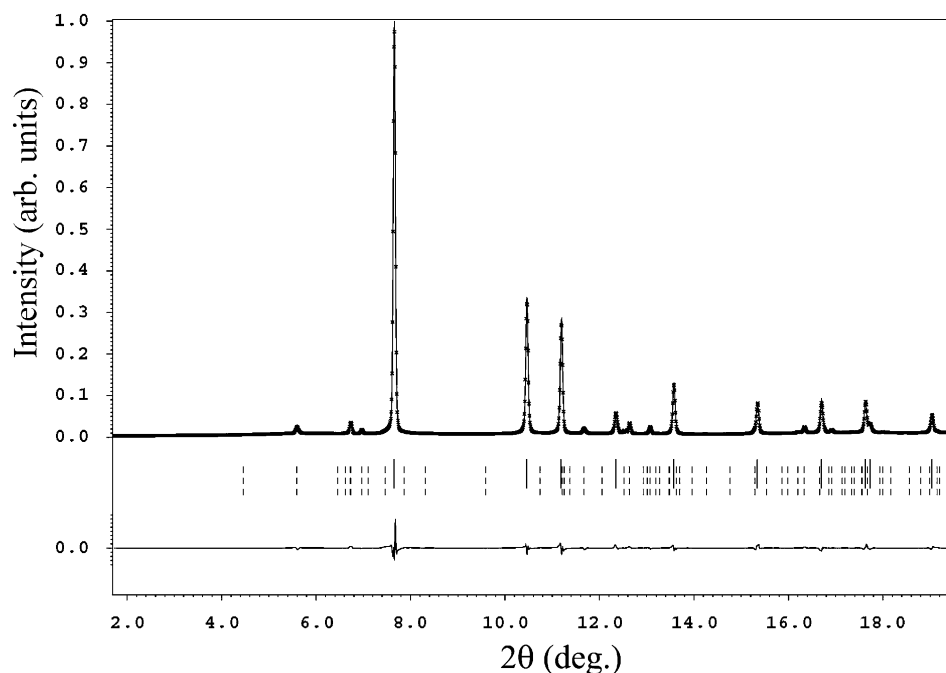


Figure 4 Observed (+) and calculated (black line) X-ray diffraction profiles for Sb_8Te_3 at 831 K by the four-dimensional Rietveld analysis. The reflection positions are indicated by vertical spikes below the diffraction patterns (black solid line: the fundamental reflection, gray broken line: the superstructure reflection). A difference curve (observed – calculated) is shown at the bottom.

temperature, finally reaching 1.638 at 831 K (this temperature is very close to the melting point). This result strongly implies that this Sb_8Te_3 sample acquired a homologous 11-layer stacking structure.

A four-dimensional Rietveld analysis of each set of diffraction data was performed using a two-atom model (Lind & Lidin, 2003). Experimental details are given in Table 1.¹ This model used the Crenel functions as the occupancy parameters of Sb and Te atoms, which means that these atoms were perfectly ordered at the arrangement in the approximated three-dimensional unit cell, and only primary (first order) modulation waves were applied to the displacements of these atoms along the z direction. The results at 831 K, the highest temperature examined in this experiment, are shown in Figs. 3 and 4, and listed in Table 2. Satellite reflections were taken into account to the third order (because refinements in which the higher-order satellites were included provided little improvement in the rate of convergence).

Fig. 5 shows the analyzed structure projected onto a three-dimensional section in which the atomic layers were extended up to 11. There was atomic displacement along the stacking direction reflecting the modulation obtained in the four-dimensional structural analysis (the alternating short- and long-layer spacings along the c direction reflecting Sb–Sb bonds). As shown in this figure, two-layer Sb–Sb blocks and

¹ Supplementary data for this paper are available from the IUCr electronic archives (Reference: SO5052). Services for accessing these data are described at the back of the journal.

five-layer Te–Sb–Te–Sb–Te blocks were repeated as $(\text{Sb–Sb})_3(\text{Te–Sb–Te–Sb–Te})$ along the c axis, and were identical to the 11-layer homologous structure (Kifune *et al.*, 2005). The coordinates projected from the four-dimensional structural analysis at 831 K and at all temperatures during the cooling process shown in Fig. 2 were almost identical to those obtained by the previous three-dimensional analysis. In the 11-layer three-dimensional structure, the modulation period γ should be calculated with $18/11 (= 1.636)$, but was 1.638 in this experiment. We presume that this slight difference resulted from compositional variation in the specimen.

The composition measured by EPMA was 28.5 at% Te, which is slightly richer in Te than the stoichiometric Sb_8Te_3 composition, and the γ value also shifted to a slightly larger value. As shown in Fig. 2, early in the heating process, the Sb_8Te_3 specimen transformed

from the amorphous phase to a disordered A7-like structure. Fig. 6 shows temperature dependences of the average spacings of three kinds of blocks. It is observed that the value of Sb_L is increasing from the others considerably with temperature. This shows that the interval of the Sb–Sb block becomes large with temperature. It is considered that this growth is caused by dissolving the vacancies in Sb layers, merging with the layers during heat treatment. Layer sequence between Te–Sb–Te–Sb–Te(NaCl) blocks changes with increasing temperature as shown below.

~450K
 Te-Sb-Te-Sb-(Sb,□)-(Sb,□)-(Sb,□)-(Sb,□)-(Sb,□)-(Sb,□)-(Sb,□)-Sb-Te-Sb-Te 15L

~600K
 Te-Sb-Te-Sb- Sb -(Sb,□)-(Sb,□)-(Sb,□)-(Sb,□)-Sb- Sb -Te-Sb-Te 13L

~700K
 Te-Sb-Te-Sb- Sb -Sb- Sb -Sb- Sb -Te-Sb-Te 11L

The typical three structural models are shown here, where □ indicates vacancies.

Increasing the temperature then caused atomic displacement, dissolving remnant vacancies and atomic ordering in the crystal, which gradually changed the c -axis length (the atomic layer spacing along the stacking direction) and the modulation period γ . Finally the sample converged to the aforementioned 11-layer structure. For this Sb–Te compound the structure and modulation period clearly changed during heat treatment.

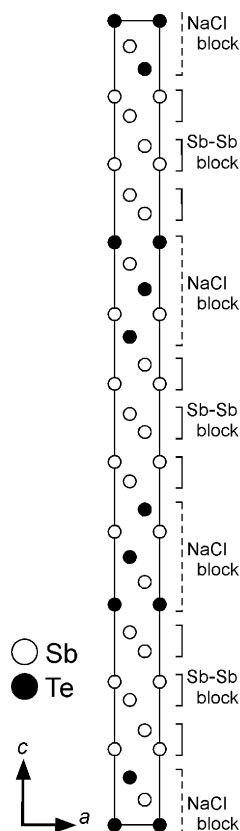


Figure 5
Projected structure onto a three-dimensional section: the atomic positions (Sb: open circle, Te: filled circle) at 831 K.

Therefore, any structural study of this system must consider both the composition and temperature of the specimen. We intend to examine other Sb–Te specimens to investigate the dependence of structure on composition. Besides the present Sb–Te compounds, the Bi–Te binary system and the GeTe–Sb₂Te₃ or GeTe–Bi₂Te₃ pseudobinary systems also form

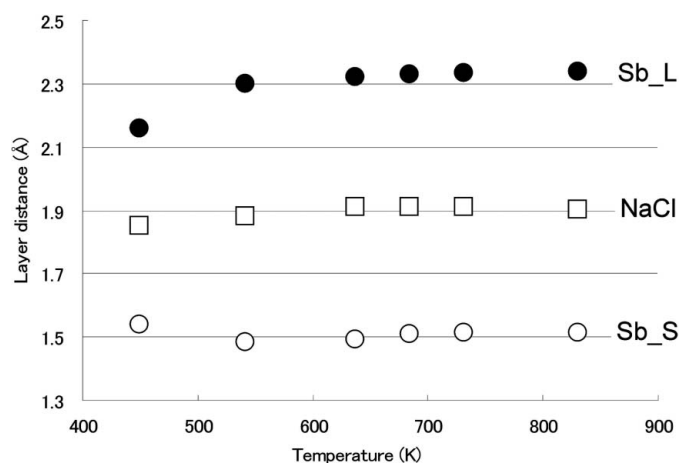


Figure 6
Temperature dependences of the average spacings of three kinds of blocks. Filled and open circles show the average values of long (Sb_L) and short spacings (Sb_S) between adjacent Sb layers, respectively. Open squares show the average spacing between Sb and Te layers in a Te–Sb–Te(NaCl) block.

various intermetallic compounds represented by the chemical formula (Bi₂)_n(Bi₂Te₃)_m, (GeTe)_n(Sb₂Te₃)_m or (GeTe)_n–(Bi₂Te₃)_m (*n*, *m*: integer). We will investigate these compounds in the future.

4. Conclusions

Our investigation revealed that the structure of a sputtered Sb₈Te₃ film specimen was amorphous, but that heating the sample caused it to crystallize into a homologous structure. After the crystallization, remarkable temperature dependencies of the lattice parameters and the modulation period were clearly observed. The crystal structure is based on the cubic close-packed stacking structure and is modulated by sinusoidal displacement waves along the stacking direction. A three-dimensional projection of the structure consists of two kinds of structural units: two layers of Sb, and five layers of Sb and Te.

The synchrotron radiation experiments were performed on BL02B2 at SPring-8 with the approval of the Japan Synchrotron Radiation Research Institute (JASRI) (Proposal Nos 2006A1649, 2006B1574, 2008A0096, 2008A1315 and 2009B0084). We express our sincere gratitude to Drs K. Kato and J. Kim at JASRI.

References

Karpinsky, O. G., Shelimova, L. E., Kretova, M. A. & Fleurial, J.-P. (1998). *J. Alloys Compd.* **268**, 112–117.
 Kifune, K., Kubota, Y., Matsunaga, T. & Yamada, N. (2005). *Acta Cryst.* **B61**, 492–497.
 Lind, H. & Lidin, S. (2003). *Solid State Sci.* **5**, 47–57.
 Matsunaga, T., Akola, J., Kohara, S., Honma, T., Kobayashi, K., Ikenaga, E., Jones, R. O., Yamada, N., Takata, M. & Kojima, R. (2011). *Nat. Mater.* **10**, 129–134.
 Matsunaga, T., Kojima, R., Yamada, N., Fujita, T., Kifune, K., Kubota, Y. & Takata, M. (2010). *Acta Cryst.* **B66**, 407–411.
 Matsunaga, T., Kojima, R., Yamada, N., Kifune, K., Kubota, Y. & Takata, M. (2007). *Appl. Phys. Lett.* **90**, 161919, 1–3.
 Matsunaga, T., Morita, H., Kojima, R., Yamada, N., Kifune, K., Kubota, Y., Tabata, Y., Kim, J.-J., Kobata, M., Ikenaga, E. & Kobayashi, K. (2008). *J. Appl. Phys.* **103**, 093511, 1–9.
 Matsunaga, T., Umetani, Y. & Yamada, N. (2001). *Phys. Rev. B*, **64**, 184116, 1–7.
 Matsunaga, T. & Yamada, N. (2004). *Phys. Rev. B*, **69**, 104111, 1–8.
 Matsunaga, T., Yamada, N. & Kubota, Y. (2004). *Acta Cryst.* **B60**, 685–691.
 Nishibori, E., Takata, M., Kato, K., Sakata, M., Kubota, Y., Aoyagi, S., Kuroiwa, Y., Yamakata, M. & Ikeda, N. (2001). *Nucl. Instrum. Methods Phys. Res. A*, **467–468**, 1045–1048.
 Petříček, V. & Dušek, M. (2000). *JANA2000*. Institute of Physics, Prague, Czech Republic.
 Poudeu, P. F. P. & Kanatzidis, M. G. (2005). *Chem. Commun.* pp. 2672–2674.
 Shelimova, L. E., Karpinskii, O. G., Konstantinov, P. P., Kretova, M. A., Avilov, E. S. & Zemskov, V. S. (2001). *Inorg. Mater.* **37**, 342–348.
 Shelimova, L. E., Karpinskii, O. G., Zemskov, V. S. & Konstantinov, P. P. (2000). *Inorg. Mater.* **36**, 235–242.
 Yamada, N. & Matsunaga, T. (2000). *J. Appl. Phys.* **88**, 7020–7028.